The Astrophysical Journal Letters, 725:L34–L37, 2010 December 10 doi:10.1088/2041-8205/725/1/L34

ATMOSPHERIC IMAGING ASSEMBLY MULTITHERMAL LOOP ANALYSIS: FIRST RESULTS

J. T. Schmelz[1,2], J. A. Kimble[1], B. S. Jenkins[1], B. T. Worley[1], D. J. Anderson[1], S. Pathak[1], and S. H. Saar[2]
[1] Physics Department, University of Memphis, Memphis, TN 38152, USA; jschmelz@memphis.edu
[2] Harvard-Smithsonian Center for Astrophysics, 60 Garden Street, Cambridge, MA 02138, USA
Received 2010 September 24; accepted 2010 October 19; published 2010 November 17

ABSTRACT

The Atmospheric Imaging Assembly (AIA) on board the *Solar Dynamics Observatory* has state-of-the-art spatial resolution and shows the most detailed images of coronal loops ever observed. The series of coronal filters peak at different temperatures, which span the range of active regions. These features represent a significant improvement over earlier coronal imagers and make AIA ideal for multithermal analysis. Here, we targeted a 171 Å coronal loop in AR 11092 observed by AIA on 2010 August 3. Isothermal analysis using the 171-to-193 ratio gave a temperature of log $T \approx 6.1$, similar to the results of Extreme ultraviolet Imaging Spectrograph (EIT) and *TRACE*. Differential emission measure analysis, however, showed that the plasma was multithermal, not isothermal, with the bulk of the emission measure at log $T > 6.1$. The result from the isothermal analysis, which is the average of the true plasma distribution weighted by the instrument response functions, appears to be deceptively low. These results have potentially serious implications: EIT and *TRACE* results, which use the same isothermal method, show substantially smaller temperature gradients than predicted by standard models for loops in hydrodynamic equilibrium and have been used as strong evidence in support of footpoint heating models. These implications may have to be re-examined in the wake of new results from AIA.

Key words: Sun: corona – Sun: fundamental parameters – Sun: UV radiation

Online-only material: color figures

1. INTRODUCTION

One of the forces driving recent scientific studies of the solar atmosphere has been the so-called coronal loop controversy. Part of this controversy has involved the conflicting results that have appeared in the literature over the past decade on coronal loop temperatures: are loops isothermal or multithermal? Is the observed loop a single flux tube or a collection of tangled magnetic strands? These questions helped inspire a series of successful workshops held in Paris (2002 November), Palermo (2004 September), Santorini (2007 June), Florence (2009 June), and coming soon, Majorca (Summer 2011).

Studies of loop temperatures from extreme ultraviolet (EUV) imagers like the EUV Imaging Telescope (EIT) on *Solar and Heliospheric Observatory* (*SOHO*) used primarily the 171-to-193 filter ratio (see, e.g., Aschwanden et al. 1999). This analysis assumed that the plasma along each line of sight was isothermal. EUV spectrometers like the Coronal Diagnostic Spectrometer (CDS) on *SOHO*, on the other hand, showed that loops were multithermal along each line of sight (Schmelz et al. 2001; Schmelz & Martens 2006). Each instrument, however, had limitations. EIT had better spatial resolution but poor temperature coverage; most analyses were limited to the isothermal approximation. CDS had excellent temperature coverage but poor spatial resolution; there was always the possibility that any given pixel could contain multiple loop structures of different temperatures. Results from the next generation of instruments added fuel to the controversial fire. The *Transition Region and Coronal Explorer* (*TRACE*) had state-of-the-art spatial resolution: 0.5 arcsec pixels and 1 arcsec resolution, but the temperature coverage was similar to that of EIT; the results from the 171-to-193 filter ratio were also similar (Lenz et al. 1999). The spatial resolution of the EUV Imaging Spectrograph (EIS) (1 arcsec pixels and 2 arcsec resolution) on *Hinode* was a vast improvement over CDS, but still no match for *TRACE*. The loops were still multithermal, even in the X-ray Telescope–EIS combined analysis (Schmelz et al. 2010), and the criticism was still the same: the pixels were too big.

Martens et al. (2002) and Weber et al. (2005) attempted to reconcile these results by suggesting that using an isothermal analysis on truly multithermal plasma would give exactly the results obtained by the EIT and *TRACE* ratio analysis. What was really needed, however, was a new instrument, one with the spatial resolution of the state-of-the-art imagers and the temperature coverage that spanned the full active region range (from below log $T = 6.0$ to above log $T = 7.0$). Data from such an instrument are now available. The Atmospheric Imaging Assembly (AIA; A. M. Title et al. 2011, in preparation) on the *Solar Dynamics Observatory* was launched on 2010 February 11. In this Letter, we analyze coronal loop data taken with AIA with the hopes of shedding new light on the coronal loop controversy.

2. ANALYSIS

AIA takes full-Sun images in multiple wavelengths nearly simultaneously, with a pixel size of 0.5 arcsec, a spatial resolution of about 1 arcsec, and a cadence of about 10 s. These features allow us to image, analyze, and model evolving coronal plasma with the best combination of spatial resolution, temporal resolution, and temperature discrimination ever achieved. There are two caveats related to our analysis that need to be mentioned; this is simply because the instrument is so new. Neither the data reduction nor the calibration is considered final, but any additional corrections are expected to be minor.

AIA was designed in part to do multithermal analysis of coronal features. The properties of the six coronal filters are listed in Table 1 and described in detail by A. M. Title et al. (2011, in preparation). Each narrowband filter is centered on a bright spectral line with a different peak formation temperature. Two of the filters, 131 Å and 193 Å also contain hot lines. These

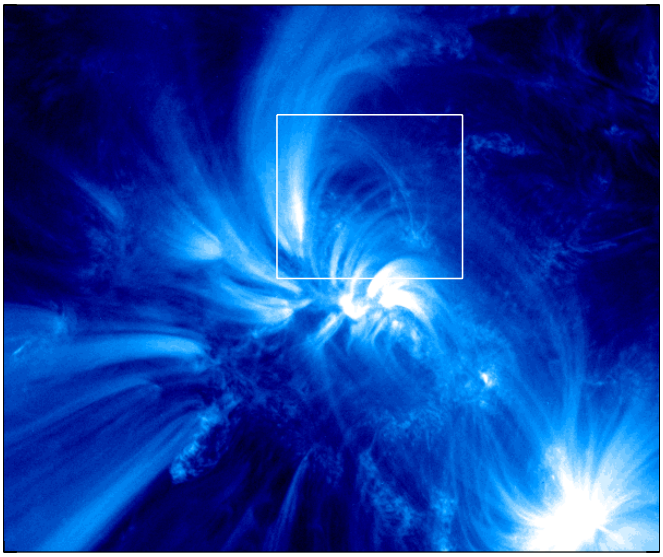

Figure 1. AIA 171 Å image of AR 11092 as observed on 2010 August 3. The main ion contributing to this filter is Fe IX with a peak formation temperature of log $T = 5.8$. The box shows the limited field of view displayed in Figure 2.
(A color version of this figure is available in the online journal.)

Table 1
AIA Observations

Filter	Primary Ion	log T	Time (UT)
131	Fe VIII (XX, XXIII)[a]	5.6 (7.0, 7.2)[a]	18:00:34
171	Fe IX	5.8	18:00:37
193	Fe XII (XXIV)[a]	6.1 (7.3)[a]	18:00:44
211	Fe XIV	6.3	18:00:37
335	Fe XVI	6.4	18:00:40
94	Fe XVIII	6.8	18:00:32

Note. [a] These filters also have high-temperature flare lines, which should not affect our analysis.

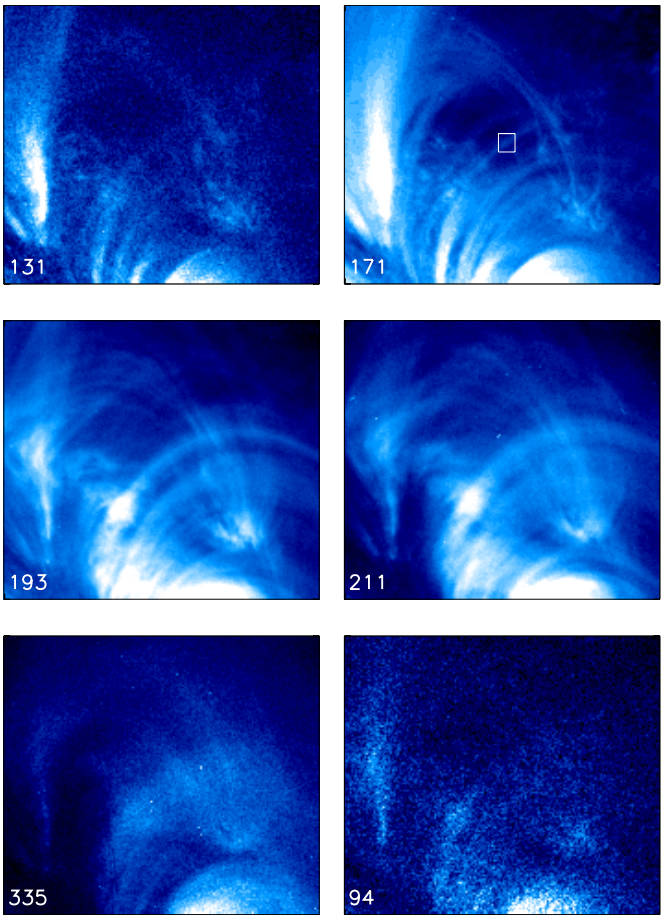

Figure 2. AIA images of a portion of AR 11092 showing the loop as seen through different filters with different temperature responses: 131 Å Fe VIII (log $T = 5.6$); 171 Å Fe IX (log $T = 5.8$); 193 Å Fe XII (log $T = 6.1$); 211 Å Fe XIV (log $T = 6.3$); 335 Å Fe XVI (log $T = 6.4$); 94 Å Fe XVIII (log $T = 6.8$). The loop segment is outline in the 171 Å image. Note that there are also high-temperature Fe XX, XXIII (log $T = 7.0$, 7.2) lines in the 131 Å channel and Fe XXIV (log $T = 7.3$) lines in the 193 Å channel, but these lines make no contributions to non-flaring active regions like the one observed here.
(A color version of this figure is available in the online journal.)

are unlikely to affect our data since the emission measure (EM) of any hot plasma (log $T \geqslant 7.0$) from quiescent active regions is likely to be several orders of magnitude down from the main peak (Schmelz et al. 2009).

Figure 1 shows the 171 Å image of AR 11092, which was located at N16W04 on 2010 August 3. The box outlines the more limited field of view used in Figure 2, which illustrates a section of AR 11092 in all the coronal filters. The loop was selected using the 171 Å image and is clearly visible in the 193 Å and 211 Å images. It is barely visible at 131 Å and 335 Å, but not visible at all at 94 Å. The loop of interest is outlined in the upper right panel of Figure 2. After co-aligning the data, we chose 10 pixels along the spine of the loop and 10 pixels from a clean background area. We averaged the loop- and background-pixel values and calculated standard deviations. Then we subtracted the background and propagated the errors. Each background-subtracted average and uncertainty were then normalized by the exposure time for the appropriate filter, resulting in units of data numbers s^{-1}. Note that since our analysis requires background subtraction, statistical errors dominate the uncertainties, including preliminary estimates of the photometric errors, which were provided by P. Boerner (2010, private communication).

Figure 3(a) shows the response of each AIA filter from Solarsoft. These curves show the sensitivity of each channel to optically thin plasma as a function of temperature. The broad temperature coverage from below log $T = 6.0$ to above log $T = 7.0$ is one of the new and important features that makes AIA the ideal instrument for multithermal analysis. The observed flux in each channel can be modeled using the appropriate response and the plasma differential emission measure (DEM):

$$\begin{aligned} \text{Flux} &= \sum \text{Response(T)} \times \text{DEM(T)}\,\Delta\,\text{T} \\ &\approx \text{Response(T)} \times \text{EM}, \end{aligned} \quad (1)$$

where the last approximation applies only if the observed plasma along the line of sight is isothermal. Using the 171-to-193 flux ratio, which was used routinely for EIT and *TRACE* loops:

$$\frac{\text{Flux}_{171}}{\text{Flux}_{193}} = \frac{\text{Resp}_{171}(\text{T})}{\text{Resp}_{193}(\text{T})}. \quad (2)$$

The results from the isothermal analysis are shown in Figure 3(b), where the curved line is the 171-to-193 instrument response ratio as a function of temperature and the flat line shows the 171-to-193 average background-subtracted flux ratio from the observations. The intersection is the resulting temperature of the (assumed) isothermal plasma. Note that there are

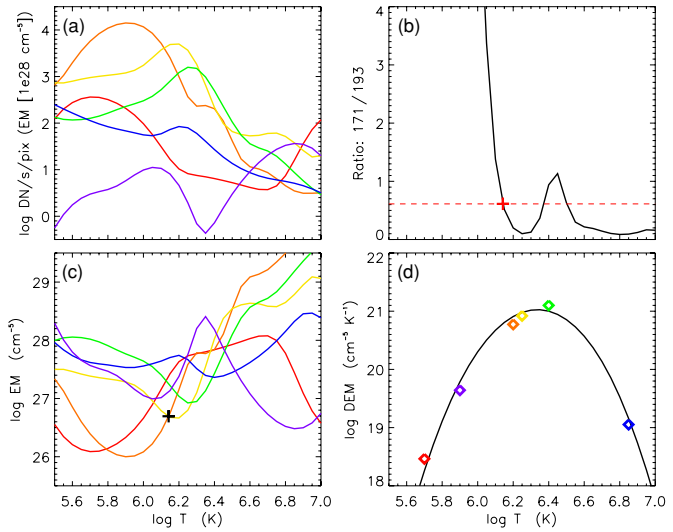

Figure 3. AIA analysis with 131 Å (red), 171 Å (orange), 193 Å (yellow), 211 Å (green), 335 Å (blue), and 94 Å (purple); (a) AIA response curves from Solarsoft showing the temperature sensitivity of the different filters; (b) isothermal analysis for the 171-to-193 ratio. The curved line shows the instrument response ratio and the flat line shows the observed flux ratio. The intersection (red plus sign) is the (assumed) isothermal temperature; (c) EM loci. Each curve represents the observed loop flux divided by the appropriate response function. The black plus sign shows the temperature and emission measure that results from the analysis in (b); (d) DEM result from DEM_interactive. The colored diamonds are the results for the different AIA filters plotted at the peak response temperature (see Table 1).

(A color version of this figure is available in the online journal.)

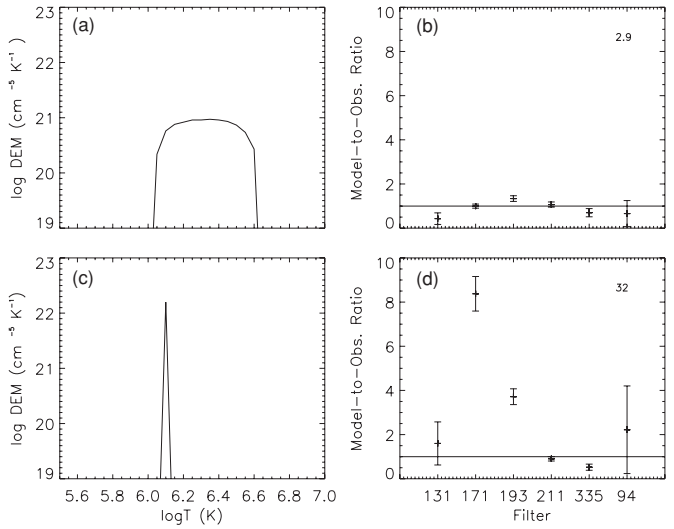

Figure 4. DEM results from DEM_manual. Top panels show the best-fit DEM and the ratios of the DEM modeled-to-observed fluxes for each AIA filter, in order of the peak response function, from lowest to highest. The value of the reduced χ^2 is printed in the upper right corner. Bottom panels show the isothermal results. Note the bad fit for the ratios and the unacceptably high value of the reduced χ^2.

also higher-temperature intersections, which are equally likely but often ignored in older EIT and *TRACE* analysis (see, e.g., the IDL routines used for calculating temperature, EIT_temp and TRACE_TEEM, in Solarsoft). Although we do not find this to be a convincing argument, the reason often given for the use of this limited range was that the 171 Å and 193 Å channels were more sensitive at these lower temperatures. This result from our analysis ($\log T \approx 6.1$, although the higher-temperature intersections are in better agreement with our multithermal analysis—see below) is the same as the alarmingly consistent results for the 171-to-193 analysis of EIT and *TRACE* loop data, which was pointed out by Schmelz et al. (2003). Unlike its predecessors, however, AIA has multiple higher- and lower-temperature coronal filters, and we can use these data to confirm or refute the isothermal results.

An EM loci plot for these data is shown in Figure 3(c). This result uses the isothermal approximation from Equation (1) and plots the background-subtracted loop flux divided by the appropriate instrument response curve. If all the curves intersected, within the uncertainties, at $\log T \approx 6.1$, then we could conclude (with reasonable confidence given the broad temperature response range of AIA) that the loop plasma is isothermal. Since the curves do not intersect at $\log T \approx 6.1$ or any other single point or even cluster at any one temperature, we are forced to conclude that the isothermal approximation made in both the ratio analysis and the EM loci analysis is too limiting. We must drop this approximation and do a full DEM analysis.

This Letter uses two different DEM analysis techniques, each with its strengths and weaknesses. The first, DEM_manual.pro, is a forward folding method with a manual manipulation of the DEM. Although this method is time consuming, it forces the user to understand both the limitations of the data as well as the assumptions going into the analysis. No smoothing is required beyond that imposed by the resolution of the instrument response functions (0.05 dex) and no a priori shape (Gaussian or double Gaussian, for example) is imposed on the final DEM curve. The second, DEM_interactive, is an automatic method built around mpfit.pro, a well-known and much-tested IDL routine that performs a Levenberg–Marquardt least-squares minimization (Levenberg 1944; Marquardt 1963). DEM_interactive is described by Warren (2005) and Brooks & Warren (2006). This method is fast and objective. The DEM curve is represented with a series of spline knots that can be repositioned interactively. In both cases, the best fit is determined from a χ^2 minimization of the differences between the observed and predicted AIA loop fluxes.

Figure 3(d) shows our results from DEM_interactive. The distribution is not consistent with isothermal plasma. The peak is not at $\log T \approx 6.1$, but between $\log T = 6.3$ and 6.4. It appears that the result from 171-to-193 ratio analysis, which is the average of the true plasma distribution weighted by the instrument response functions, is deceptively low. Figure 4 shows our results from DEM_manual. The top panels are for the best-fit result, which gives the lowest value of the reduced χ^2. Note that the overall shape and peak of the distribution agree well with the results shown in Figure 3(d). We also plot the ratios of the DEM modeled-to-observed fluxes for each of the AIA filters. All the ratios are within 1σ–1.5σ of one, indicating an excellent fit to the data. We contrast these with the results in the bottom row, where the DEM is a single narrow distribution that peaks at $\log T = 6.1$. We changed the height of this distribution to minimize the reduced χ^2, but note the bad fit for the ratios in the lower right panel, including the unacceptably high value of the reduced χ^2.

3. DISCUSSION

Our results imply that the loop segment under investigation is multithermal, with a distribution that is neither narrow nor extremely broad, where the bulk of the EM is $6.1 < \log T < 6.6$. This temperature distribution is similar to those determined

for other loops using spectroscopy data (see, e.g., Schmelz & Martens 2006; Schmelz et al. 2010). These results have potentially serious implications: the isothermal approximation not only gave a deceptively low temperature, but also gave a value that agreed with the overwhelming majority of isothermal approximation results from 171-to-193 ratio analysis of EIT and *TRACE*. These EIT and *TRACE* results show substantially smaller temperature gradients than predicted by standard models for loops in hydrodynamic equilibrium (see, e.g., Lenz et al. 1999; Aschwanden et al. 2001) and have been used as strong evidence in support of footpoint heating models. We note, however, that recent coronal loop models by, e.g., Bourouaine et al. (2008) consider weak collisions and non-thermal properties of the coronal loops and predict that footpoint heating produces a small temperature gradient along the loop.

Our results verify the predictions of Martens et al. (2002) and Weber et al. (2005) who theorized that the alarmingly consistent EIT and *TRACE* 171-to-193 ratio values ($\log T \approx 6.1$) were the result of multithermal plasma. These predictions have also been supported by recent *Hinode* EIS spectroscopic observations (e.g., Tripathi et al. 2009) as well as simulated *TRACE*/EIT multi-strand coronal loop modeling (e.g., Sarkar & Walsh 2009; Bourouaine & Marsch 2010). These results show that even *TRACE*/EIT triple-filter analysis cannot determine whether the loop segments are isothermal or multithermal, especially when the estimated photometric errors are relatively high.

Of course, the analysis presented here is for just one loop, and more work needs to be done before we can reach a definitive conclusion. Also, we have not yet looked at the DEM results for different positions along the loop, so we cannot yet say anything about temperature gradients or the likelihood of footpoint heating. We are working on both of these issues: expanding our data set with DEM results of more loops from both the same and different active regions and also analyzing areas along the loops, from footpoint to peak, to see if we can detect temperature gradients that may or may not conform to different heating models.

AIA was designed in part to do multithermal analysis of coronal features. Our results show that the instrument is working as expected, and that AIA may, in the not too distant future, finally resolve the isothermal versus multithermal component of the coronal loop controversy.

We thank Mark Weber, Ed Deluca, and Leon Golub of SAO for help with the AIA data. The Atmospheric Imaging Assembly on the Solar Dynamics Observatory is part of NASA's Living With a Star program. Solar physics research at the University of Memphis is supported by NSF ATM-0402729 as well as a *Hinode* subcontract from NASA/SAO.

REFERENCES

Aschwanden, M. J., Newmark, J. S., Delaboudinire, J.-P., Neupert, W. M., Klimchuk, J. A., Gary, G. A., Portier-Fozzani, F., & Zucker, A. 1999, ApJ, 515, 842
Aschwanden, M. J., Schrijver, C. J., & Alexander, D. 2001, ApJ, 550, 1036
Bourouaine, S., & Marsch, E. 2010, ApJ, 708, 1281
Bourouaine, S., Vocks, C., & Marsch, E. 2008, ApJ, 676, 1346
Brooks, D. H., & Warren, H. P. 2006, ApJS, 164, 202
Lenz, D. D., DeLuca, E. E., Golub, L., Rosner, R., & Bookbinder, J. A. 1999, ApJ, 517, L155
Levenberg, K. 1944, Q. Appl. Math., 2, 164
Marquardt, D. 1963, SIAM J. Appl. Math., 11, 431
Martens, P. C. H., Cirtain, J. W., & Schmelz, J. T. 2002, ApJ, 577, L115
Sarkar, A., & Walsh, R. W. 2009, ApJ, 699, 1480
Schmelz, J. T., Beene, J. E., Nasraoui, K., Blevins, H. T., Martens, P. C. H., & Cirtain, J. W. 2003, ApJ, 599, 604
Schmelz, J. T., & Martens, P. C. H. 2006, ApJ, 636, L49
Schmelz, J. T., Saar, S. H., DeLuca, E. E., Golub, L., Kashyap, V. L., Weber, M. A., & Klimchuk, J. A. 2009, ApJ, 693, L131
Schmelz, J. T., Saar, S. H., Nasraoui, K., Kashyap, V. L., Weber, M. A., DeLuca, E. E., & Golub, L. 2010, ApJ, 723, 1180
Schmelz, J. T., Scopes, R. T., Cirtain, J. W., Winter, H. D., & Allen, J. D. 2001, ApJ, 556, 896
Tripathi, D., Mason, H. E., Dwivedi, B. N., del Zanna, G., & Young, P. R. 2009, ApJ, 694, 1256
Warren, H. P. 2005, ApJS, 157, 147
Weber, M. A., Schmelz, J. T., DeLuca, E. E., & Roames, J. K. 2005, ApJ, 635, L101